The Cryogenic AntiCoincidence detector for ATHENA X-IFU: the project status.

C. Macculi 1 • A. Argan 1 • D. Brienza 1 • M. D'Andrea 1 • S. Lotti 1 • G. Minervini 1 • L. Piro 1 • M. Biasotti 2 • L. Ferrari Barusso 2 • F. Gatti 2 • M. Rigano 2 • G. Torrioli 3 • M. Fiorini 4 • S. Molendi 4 • M. Uslenghi 4 • E. Cavazzuti 5 • A. Volpe 5

1 INAF/IAPS Roma, Italy
2 University of Genova, Dept. of Physics, Italy
3 CNR/IFN Roma, Italy
4 INAF/IASF Milano, Italy
5 ASI Roma, Italy

Abstract The ATHENA observatory is the 2nd large class ESA mission to be launched on 2031 at L2 orbit. One of the two on board instruments is X-IFU, a TES based kilo-pixels array able to perform simultaneous high-grade energy spectroscopy (FWHM 2.5eV@7keV) and imaging over the 5' Field of View. The X-IFU sensitivity is degraded by primary particles background of both solar and Galactic Cosmic Rays (GCR) origin, and by secondary electrons produced by primaries, interacting with the materials surrounding the detector: these particles cannot be distinguished by the scientific photons, thus degrading the instrument performance. Results from studies regarding the GCR component performed by Geant4 simulations address the necessity to use background reduction techniques to enable the study of several key science topics. This is feasible by combining an active Cryogenic AntiCoincidence detector (CryoAC) and a passive electron shielding to reach the required residual particle background of 0.005 cts/cm^2/s/keV inside the 2-10 keV scientific energy band. The CryoAC is a 4 pixel detector made of Si suspended absorbers sensed by a network of IrAu TESes, and placed at a distance < 1 mm below the TES-array.
Here we will provide an overview of the CryoAC program, starting with some details on the background assessment having impacts on the CryoAC design, then we continue with its design concept including electronics, and the Demonstration Model results, to conclude with programmatic aspects.

Keywords ATHENA X-IFU • Anticoincidence detectors • TES

1 Introduction

The ATHENA mission [1] has been conceived to provide exhaustive answers to the following astrophysical questions: How does ordinary matter assemble into the large-scale structures we see today? How do black holes grow and shape the Universe? The result is a satellite having on-board two complementary instruments: the X-IFU [2] and the WFI [3]. The X-IFU will provide: a) 3D integral field spectroscopic mapping of hot cosmic plasmas, enabling measurements of gas bulk motions and turbulence, chemical abundances and the spatial distribution of these and other physical parameters; b) Weak spectroscopic line detection, enabling the detection of unresolved absorption and emission lines from Warm and Hot Intergalactic Medium filaments and weak spectral features produced by unusual ion species or states; c) Physical characterization of the Hot and Energetic Universe, including plasma diagnostics using emission line multiplets, AGN reverberation and black hole spin measurements, winds in galactic sources in outburst, AGN winds and outflows, stellar outflows, solar wind charge exchange, etc. The WFI in the survey mode will provide: a) the access to a new discovery space for supermassive black holes; b) the identification of distant galaxy groups and clusters, thus allowing to measure their gas entropy profiles on all mass scales out to z~2; c) temperature maps of clusters around radio-loud AGN out to intermediate redshifts. It will also map shock structures, will test jet evolution models and will infer their impact at the epoch of group and cluster formation.

In particular, one of the X-IFU scientific aims, the reference instrument along this paper, is to provide high spectral energy resolution maps of faint or diffuse sources, thus a very low residual particle background (bkg) is required around the TES-array detector. To perform this task, it is necessary to adopt reduction techniques. So, the cryogenic X-IFU Focal Plane Assembly (FPA) will be equipped with a passive electron shielding surrounding the TES-array, and an active anticoincidence detector as the CryoAC. On February 2019, the I-PRR (Instrument-Preliminary Requirement Review) for X-IFU has been held, where we reported the CryoAC instrument definition, its design concept and related trade-off studies. At the Adoption planned on 2021, it is requested by ESA that critical subsystems must reach TRL5 (Technology Readiness Level) by Demonstration Model (DM) to enable critical technologies.

2 From BKG assessment to the CryoAC design concept

2.1 BKG assessment

In High Energy Astrophysics, the particle bkg assessment is a typical task to be pursued during Phase A of an ESA space mission lifecycle.

Title

It directly affects the instrument sensitivity, hence the instrument design: the higher the residual bkg, the lower the instrument sensitivity. The requirement foresees a residual bkg of 0.005 cts/cm^2/s/keV in 2-10 keV scientific energy band. The contribution to the bkg is mainly divided in two categories:

1) the so called "Soft Proton/ions" (E < few hundred's keV) components, whose origin is the Sun and L2 (present baseline orbit) magnetotail, that can be collimated by the ATHENA grazing incidence X-ray optics towards the FPA
2) the GCRs (hundred's MeV to GeV) that crossing the satellites over 4π sr arrive at the focal plane producing also secondaries.

While for the low energy component the plan is to use a magnetic diverter to cut away this flux of charged particles from the cryostat, to reduce the high energy GCR component it is necessary to adopt an active detection system. We remind that Minimum Ionizing Particles (MIPs), having GeV energy scale, typically deposit ~ 4-5 keV inside the X-IFU scientific energy band (the TES array absorbers are made of Bi 4.2 μm thick, and Au 1.7 μm thick). To assess the impact of the particle environment onto the TES-array, simulations by Monte Carlo method using the Geant4 toolkit have been performed [4, 5]: this primary flux interacts with the "mass model" of the payload, which is a simplified instrument environment but representative of the mass composition and distribution around the TES-array detector (from the satellite, through the cryostat, down to the detailed cryogenic FPA), to produce the expected bkg. In Fig. 1 we show the present X-IFU mass model, and the expected residual bkg by applying both reduction techniques. The electron liner made of a Kapton/Bi bi-layer, to be revised in the next phase in Kapton/Au due to manufacturing problem when handling the bismuth, is a passive shield necessary to reduce the e^- contribution towards the TES array. It has a double aims: it reduces secondary electrons produced by primaries crossing the Niobium magnetic shield (in blue), and it also generates a lower number of tertiary electrons. Moreover, without the CryoAC detector, the TES-array would experience a particle bkg ~ 40 higher than the requirement.

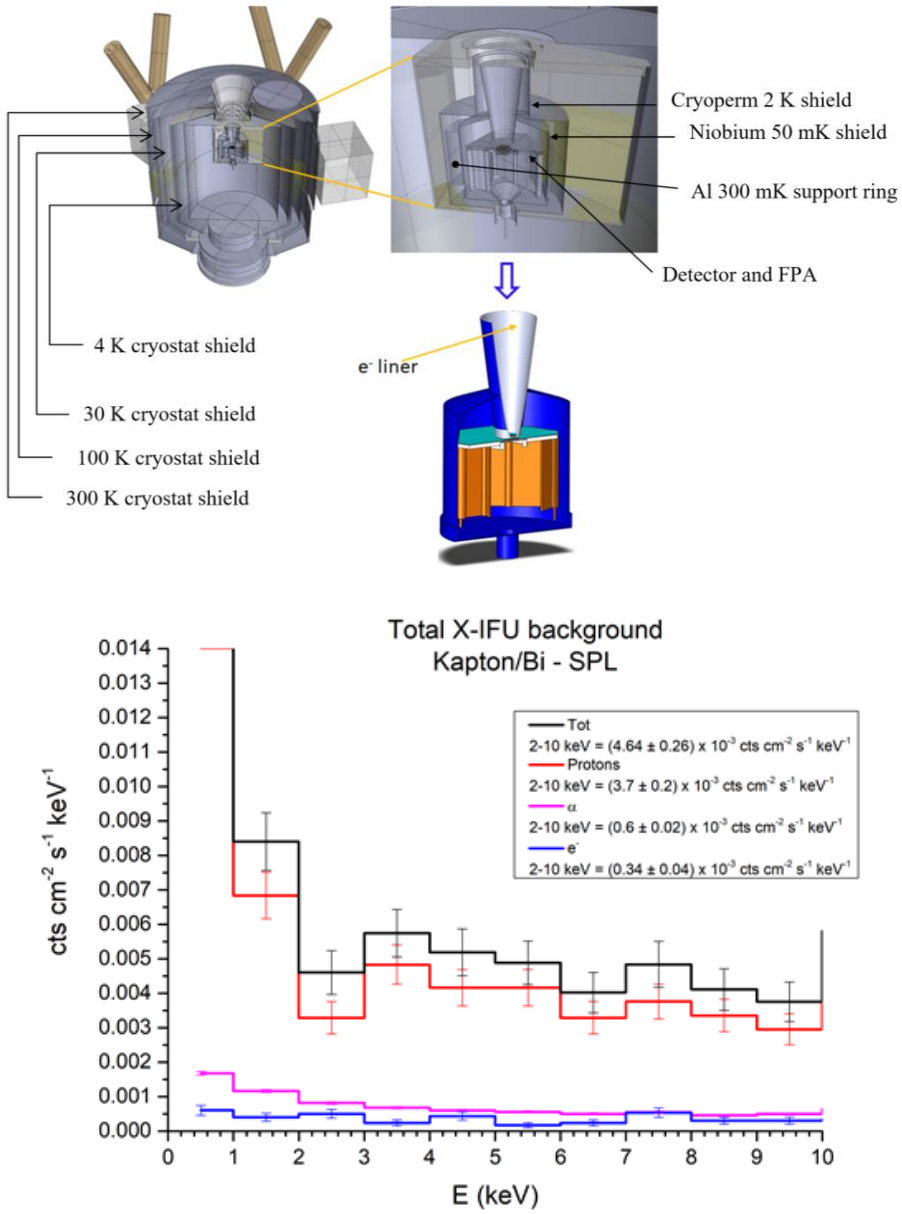

Fig. 1 *Top and Center*: the X-IFU mass model. On *Top Left*, the complete cryostat, on *Top Right* a zoom of the FPA region to highlight the detector hexagon in the center. In the *Middle* a sketch to show the electron liner shield. *Bottom*: expected residual background from the different particle species present in L2. The requirement is 0.005 cts/cm^2/s/keV (error is due to statistics, the equivalent time of the simulations is several thousands of seconds). (Color figure online).

2.2 Design concept

Main requirements and system constraints sizing the CryoAC are in Table 1:

Table 1: Main requirements and system constraints sizing the CryoAC. The acronym "CBE" means "Current Best Estimate".

Parameter	Value
Geometrical rejection efficiency	98.5%
Detection efficiency	99.98%
Allocated power dissipation	< 40 nW (CBE)
Time tagging accuracy	≤ 10 μs
Intrinsic Deadtime	1%

The main top requirements for which the CryoAC has to be compliant are: 1) the efficiency, having a direct impact onto the low energy threshold; 2) the deadtime, having a direct impact on the detector maximum energy and its time constants, and the power dissipation via the thermal conductance.
Since the CryoAC absorber is based on Si working at sub-K temperatures, the dynamic of pulse evolution after energy deposition will be led by the thermal and athermal regime. Ballistic athermal phonons can soon enter the TESes deposited on the crystal surface, quickly heating the electron gas, thus forming a first pulse. Then, the diffusive phonons will rise generating an added thermal pulse. Athermals are used as flag to rise the particle veto, thus asking for good collection for better pulse shaping. The baseline design is based on absorbers made of a thin Si crystal (0.5 mm thick), where the energy deposited by particles is sensed by a network of TES sensors (Fig. 2). The CryoAC is placed below the TES-arrays, at a distance < 1 mm. The active part covers a full area of 4.91 cm^2, larger than the TES array (2.3 cm^2).

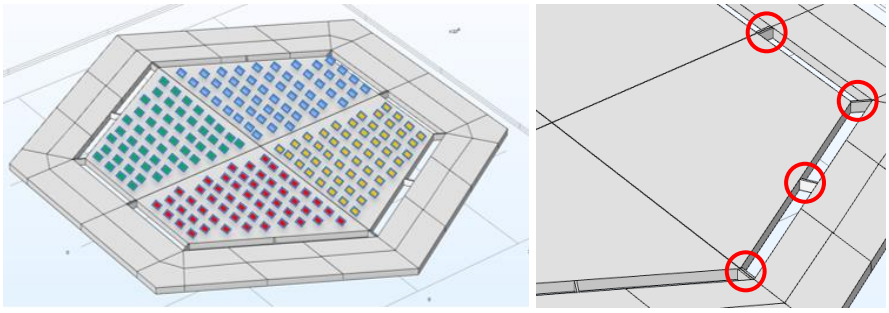

Fig. 2 CryoAC baseline configuration: 4 independent pixels. It is shown only the "concept": 4 independent TES networks, each network deposited on a separate trapezoidal absorber. Other details as, for example, wiring and pads layout, are not

shown since they are still under study. On the right, the 4 silicon beams connecting each of the 4 absorber to the silicon rim are shown. (Color figure online).

The baselined detector is divided into 4 independent pixels, each one has an area of 1.23 cm^2, and having on board a network of ~ 120 IrAu TES connected in parallel. Each pixel is connected to a gold-plated Si rim by 4 Si beams realizing the pixel thermal conductance. Each pixel-absorber will also have deposited on board Pt heaters to increase its temperature, if necessary, to decrease bias currents thus limiting magnetic coupling effects to the TES array (expected ~ 10 mA order due to the TES network high critical current). The compliance of the design to the requirements has been verified through an analysis of the system, including background assessment by Geant4 [4, 5], and tests on prototypes [7-10]. At present the baseline design which is the 4-pixels detector, is being traded-off with a monolithic hexagonal absorber to see pro and cons in terms of detector responsivity, rejection efficiency, deadtime, robustness.

As for the electronics (Fig. 3), the CryoAC will be read out using 4 SQUID channel in standard Flux Locked Loop configuration (FLL), one for each of the 4 pixels.

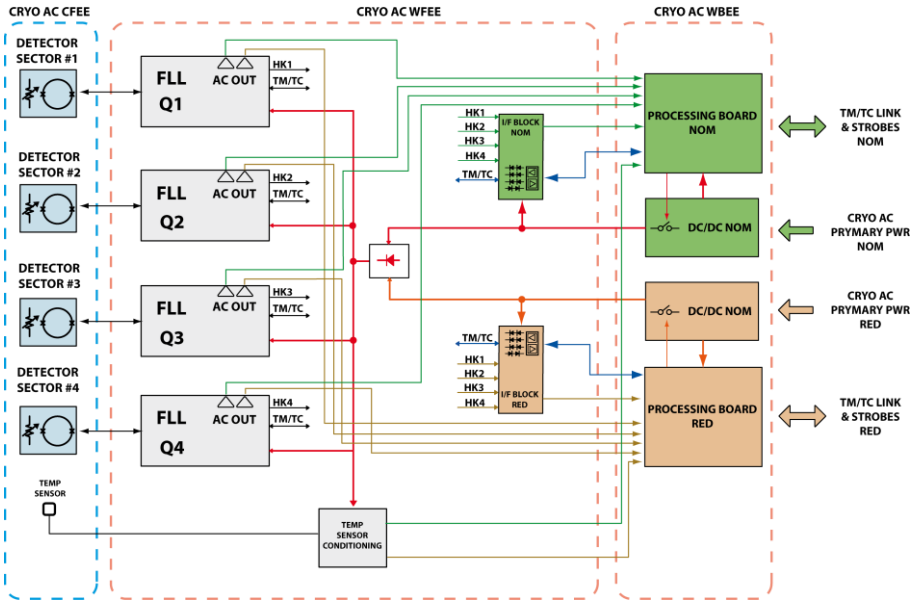

Fig. 3 The CryoAC Electronics: Cold Front End (CFEE) composed by the 4 SQUID to sense the current from the 4 pixels, Warm Front End divided in 4 Quadrant, each one providing bias to TES and SQUID single pixel and producing the analogic scientific signal (AC OUT) and the FLL HouseKeepings. On the right the Warm Back End divided in Nominal and Redundant boards, each one processing and

digitizing the signal from the WFEE, and packeting the data to be sent to the Instrument Control Unit. (Color figure online).

To be compliant with the failure management philosophy we have adopted as baseline an independent FLL chain for each "pixel + SQUID" that will be served by a so-called Quadrant service electronic section inserted in the CryoAC Warm Front End Electronics (WFEE). The Warm Back End Electronics (WBEE) will manage the WFEE, digitize its analogic output, apply quality grades and time stamps to the pulses, and organize the telemetry packet. The baseline plans veto operation on ground due the expected low telemetry rate.

3 CryoAC fabrication process

In the context of the DM, as expected for the TRL4 path which definition is "Component and/or breadboard functional verification in laboratory environment", care has been taken during all the fabrication processes (see Ref. [6] for details) (Fig. 4) that are propaedeutic for all the models to be produced (i.e., Engineering Model-EM, Qualification Model-QM, Flight Model-FM).

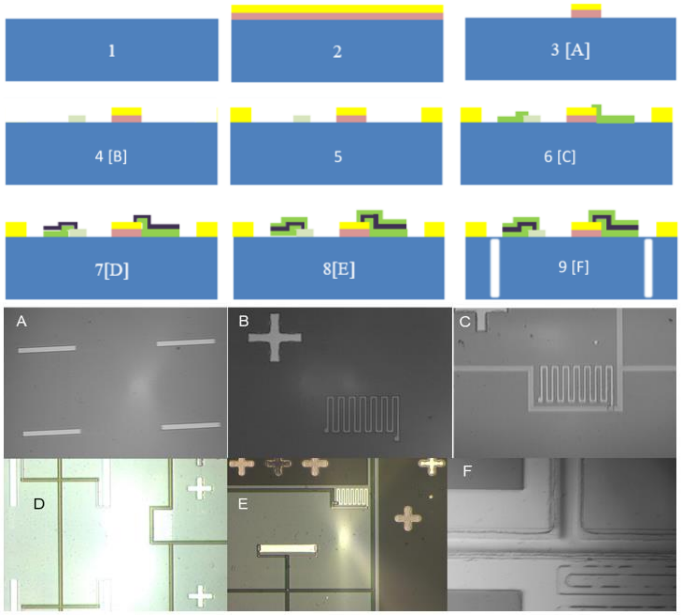

Fig. 4 Fabrication process. See text for details. (Color figure online)

Particular attention has been put on: the deposition of the IrAu defining the TES critical temperature, and the final etching of the chip. Here

is a quick description of such processes step by step: 1) Silicon wafer, 2) IrAu (240nm/80nm thick) bilayer deposition by Pulse Laser Deposition technique, 3) TES IrAu bilayer etching by ion milling, 4) Pt heaters (50 nm thick) fabrication by evaporation and lift-off, 5) Au thermalization layer (~ 230 nm thick) deposition on rim by evaporation and lift-off, 6) Niobium wiring (lower strip) fabrication by RF-sputtering and lift-off, 7) Silicon oxide insulation by evaporation and lift-off, 8) Niobium wiring (upper strip) fabrication by evaporation and lift-off, 9) Deep Reactive Ion Etching (1^{st} step - Al Hard-mask deposition; 2^{nd} step - Etching using Bosch process; 3^{rd} step - Removal aluminum mask). To summarize we have in total 7 photolithographic processes: 1 positive photolithography and etching, and 6 negative photolithography and liftoff.

It is worth noticing that Nb wiring (lower stripline ~ 490 nm, upper stripline ~ 1000 nm thick, respectively) have been overlapped in anti-inductive configuration to reduce magnetic coupling towards the TES array. The formalization of the procedures in detail is in progress, together with the revision process aimed at ensuring maximum reproducibility and at maximizing the production yield.

4 The DM CryoAC

The aim of the DM (for details see [6, 11]) is the detector functional qualification to get the TRL4, thus consolidating the path to get TRL5 consisting on the "Component and/or breadboard validation in relevant environment". Being the CryoAC a cryogenic detector, in addition to the usual thermal cycles (cooling and warming up), in the ATHENA context "relevant environment" means to test the CryoAC under mechanical vibration. The DM detector is representative of the baseline, and it is aimed at demonstrating the maturity level of the most critical technology by means of:

- qualification of the manufacturing processes (see Ref. [6] for some details)
- full knowledge of the physics ruling the detector performance (see Ref. [6-11] for details)

Once the DM program will be concluded, the next step is to vibrate the full geometry (see Fig. 2) to get TRL5.

The functional requirements to be satisfied by the DM CryoAC are: suspended pixel size (abs. area) of 1 cm^2; low energy threshold at 20 keV; operation at T_b = 50 mK; power dissipation < 40 nW. In Fig. 5 are reported some pictures and results of the AC-S10 sample that, being compliant with the DM requirement, has been defined as the "DM CryoAC".

The results are compliant with the requirements. They also show a very low energy threshold (< 3 keV) and some spectroscopic capability (~ 20%@6keV). After the stand-alone test performed in Italy, the DM has been delivered to SRON for integration at the chipset level with the TES array.

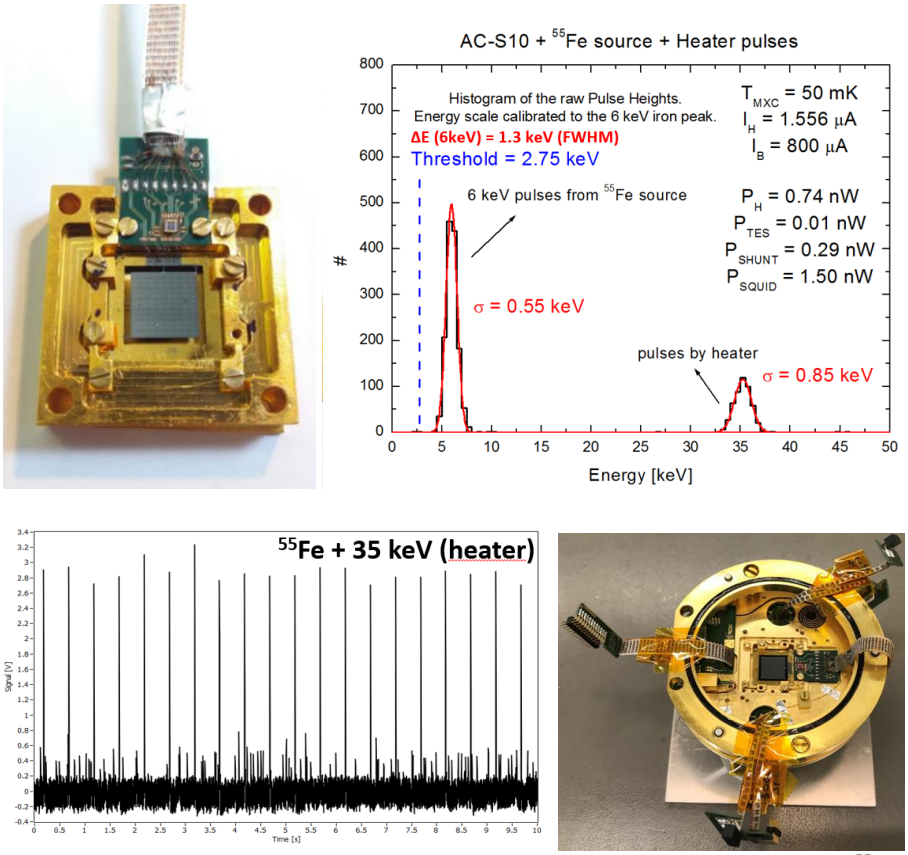

Fig. 5 *Top left* DM CryoAC in INAF holder. *Top right* Energy spectrum from ^{55}Fe, and 35 keV pulses injected by the heater. *Bottom left* Raw data stream. *Bottom right* fit-checking in the 40 PxlB flange at SRON (credits SRON). (Color figure online).

5 Near term CryoAC activities

The main near term milestones are: production of a 1st structural model (SM) to be vibrated by Fall 2019 thus having a feedback on the Si-beams, defining the absorber-to-bath thermal conductance, from the robustness point of view; the closure of a proto-EM design (a propedeutic model for the EM) by end of 2019 which is a detector having hexagonal geometry (see Fig. 2) but only 1 instrumented readout chain, to start its production in early 2020. By mid-2020, the production of a 2nd SM to get

TRL5 that with respect to the 1st one will have representative interfaces to the FPA. We are working to produce a Warm Electronics breadboard to be tested in combination with the proto-EM by end of 2020: the coupling of these 2 items is the base for the EM CryoAC design. By end 2021 we expect to close the work related to an end-to-end simulator whose main driver is the pulses production, starting from the athermal and thermal phonons physics, to be used as design tool for the electronics (trigger logic, pileup, deadtime).

Acknowledgements This work has been supported by ASI contract n. 2018-11-HH.0, ESA CTP contracts n. 4000116655/16/NL/BW and n. 4000114932/15/NL/BW, and by AHEAD H2020 project (grant n. 654215). SRON is acknowledged for the fit-checking picture.

References

1. K. Nandra, X. Barcons, D. Barret, A. Fabian, J. W. den Herder, L. Piro, M. Watson, et al., ATHENA Mission Proposal, http://www.the-ATHENA-x-ray-observatory.eu/images/ATHENAPapers/The_ATHENA_Mission_Proposal.pdf (2013).
2. D. Barret, T. Lam Trong, J.W. den Herder, L. Piro, M. Cappi, et al., Proc. SPIE 10699, 106991G (2018) doi: 10.1117/12.2312409
3. N. Meidinger, J. Eder, et al., Proc. of SPIE Vol. 9905, 99052A (2016), doi: 10.1117/12.2231604
4. S. Lotti, et al., Proc. of SPIE Vol. 10699, 106991Q (2018), doi: 10.1117/12.2313236
5. S. Lotti, et al., XIFU-INAF-BKG-TN-0002 (2019), internal Tech. Note
6. M. Biasotti, J. Low Temp. Phys. **This Special Issue** (2019)
7. C. Macculi, et al., Proc. of SPIE Vol. 9144, 91445S (2014), doi: 10.1117/12.2054946
8. M. D'Andrea, et al., Proc. of SPIE Vol. 9905, 99055X (2016), doi: 10.1117/12.2231412
9. M. D'Andrea et al., J. Low Temp. Phys **193**, 949 (2018), doi: 10.1007/s10909-018-2039-4
10. M. D'Andrea, et al., Proc. of SPIE Vol. 10699, 106994T (2018), doi: 10.1117/12.2313280
11. M. D'Andrea, J. Low Temp. Phys. **This Special Issue** (2019)